

Detailed Optical Spectroscopy of the B[e] Star MWC 17

V. G. Klochkova* and E. L. Chentsov**

Special Astrophysical Observatory, Russian Academy of Sciences, Nizhnii Arkhyz, 369167 Russia

Received June 17, 2015; in final form, July 31, 2015

Abstract—Based on the material of multiple high-resolution $R = 60\,000$ observations conducted on the 6-m telescope (BTA) of the Special Astrophysical Observatory in combination with the Nasmyth Echelle Spectrograph (NES), we closely studied the features of the optical spectrum of the star MWC 17 with the B[e] phenomenon. In the wavelength interval of 4050–6750 Å, we identified numerous permitted and forbidden emissions, interstellar Na I lines, and diffuse interstellar bands (DIBs). Radial velocities were estimated from lines of different origin. As the systemic velocity, V_{sys} , the velocity of the forbidden emissions can be accepted: -47 km s^{-1} (relative to the local standard $V_{\text{lsr}} = -42 \text{ km s}^{-1}$). Comparison of the obtained data with the earlier measurements allows us to conclude on the absence of considerable variability of spectral details.

DOI: 10.1134/S1990341316010041

Keywords: *stars: emission-line, Be—stars: individual: MWC 17*

1. INTRODUCTION

The hot B-type star MWC 17 = V832 Cas is referred to the objects with the B[e] phenomenon [1, 2]. The B[e] phenomenon involves having a number of peculiar details in the stellar spectrum: primarily, strong emission lines of neutral hydrogen H I and helium He I, emissions of the permitted lines of metal ions, and low-excited forbidden lines. The second significant feature of stars with the B[e] phenomenon is large IR flux excess due to circumstellar hot dust. However, the stars which meet these two main criteria form a group of highly heterogeneous objects. Lamers et al. [3], having developed the classification criteria for the stars with the B[e] phenomenon, divided them in five subtypes. They did not refer the star MWC 17 to any of those subtypes, it appears in publications as a member of the most populated B[e]-unclassified subgroup.

A few dozens of the unclassified stars with the B[e] phenomenon were investigated by Miroshnichenko and coauthors. The review of the results obtained, including the spectral data from the 6-m telescope, is given in [4]. One of the results of the spectroscopic investigation lies in the fact that unclassified B[e] stars are interacting binary systems in the broad range of luminosities. Objects with luminosities $L \leq 10^5 L_{\odot}$ are separated into a new group called the objects of the FS CMa type. About 30% of FS CMa-type

objects exhibit various signs of binarity. In [5], it is also suggested to consider the unclassified B[e] stars as interacting binaries.

The main problem in the investigation of stars with the B[e] phenomenon is the estimation of star's luminosity. The luminosity would allow one to detect the evolution stage of the star and range it to one or another type of hot stars with similar features in the spectra. Still, in optical spectra of the stars with the B[e] phenomenon, as a rule, one cannot find the absorptions which form in the stellar atmosphere conditions and could serve as criteria for luminosity estimation. The fact which also causes a problem is that two above mentioned distinctive features (spectral peculiarity and IR-flux excess) are intrinsic to several types of hot stars observed at the essentially different evolution stages: young Herbig Ae/Be stars, evolved massive stars of high luminosity (LBV, supergiants), and far evolved low-mass stars which are close to the planetary nebula phase.

The situation with the B-type star VES 695, which is associated with the IR source IRAS 00470+6429 and has an emission spectrum, properly illustrates the difficulties in determination of evolutionary statuses of stars with emission spectra. For a long time, this object had been considered as a possible protoplanetary nebulae (PPN) candidate at the stage close to the PN phase (see [6] and references therein). However, the complex study [7], carried out with a large volume of observation material, including the echelle spectra from the 6-m telescope, resulted

*E-mail: valenta@sao.ru

**E-mail: echen@sao.ru

in an alternate conclusion on the evolutionary status of VES 695. Complex of the obtained fundamental parameters (luminosity, characteristic features of energy distribution in the spectrum, binarity indications for the star) allowed Miroschnichenko et al. [7] to refer VES 695 to the stars of the FS CMa type.

MWC 17 which is associated with the IR source IRAS 01441+6026 is one of the hottest stars with the B[e] phenomenon. It is located near the galactic plane and has the coordinates: $\alpha(2000) = 01^{\text{h}}47^{\text{m}}38.5^{\text{s}}$, $\delta(2000) = +60^{\circ}41'57''$, $l = 129^{\circ}8$, and $b = -1^{\circ}4$. In the optical range, MWC 17 is quite a faint star with a magnitude $V = 11^{\text{m}}7$ [8]. Due to high reddening, the star is weaker in the B band, $B = 13^{\text{m}}5$ (according to the SIMBAD¹ data), thus, its optical spectrum is understudied at present. Zickgraf carried out the only spectroscopic study of MWC 17 with high spectral resolution [8]. The spectral resolution of his data (from 23 000 to 45 000) is comparable to ours, but this author used only small regions of the spectrum. The $H\alpha$, He I 5876, [N II] 6583, [O I] 6300, [S III] 6312, and [Fe II] 7155 Å profiles are presented in [8] graphically. Relative intensities and radial velocities are given for these lines as well as for He I 6678 and Na I 5890, 5896 Å.

To search for possible variability of the MWC 17 optical spectrum and to add data on its peculiarities, we conducted detailed identification and necessary measurements of the parameters of spectral details of different origin from the spectra obtained with a resolution $R = 60\,000$ in the broad wavelength range 4050–6750 Å. The observation data used is briefly described in Section 2. Section 3 presents information on the profile features of spectral details found with the high-resolution spectra, their analysis, and discussion of the results derived. In Section 4, we deal with the position of MWC 17 in the Galaxy, and the main conclusions are summed up in Section 5.

2. OBSERVED DATA

We use the MWC 17 spectra obtained on the 6-m telescope with the Nasmyth Echelle Spectrograph (NES) [9]. The spectrograph equipped with a CCD of 2048×2048 elements and an image slicer [10] provides $R = 60\,000$ in the wavelength range of 3500–6800 Å. Extraction of one-dimensional spectra from two-dimensional echelle images was conducted using the modified [11] MIDAS Echelle context. Table 1 shows the dates of obtaining the spectra and the detected spectral intervals. Correction and control of instrumental coordination of spectra of the star and the lamp with a hollow cathode were fulfilled with

Table 1. Dates of obtaining the spectra used and the detected spectral interval

Date	$\Delta\lambda$, Å	Date	$\Delta\lambda$, Å
Nov 15, 2005	5275–6735	Mar 14, 2006	4050–5450
Jan 15, 2006	4570–5980	Sep 02, 2006	5275–6735
Jan 16, 2006	4570–5980		

the telluric lines [O I], O₂, and H₂O. The procedure of radial velocity V_r determination from the spectra obtained with NES and error sources are described in more detail in [12]. The root-mean-square error of the measurements is $V_r \leq 0.8 \text{ km s}^{-1}$ for one thin line.

3. MAIN TYPES OF LINE PROFILES

As early as in the first publication, when we mentioned some features of the MWC 17 spectrum [13], a remarkably high intensity of emissions was noted. Intensity variations, from peaks of the strongest H I, [O I] emissions to the Na I absorption cores, and therefore lowering of the signal-to-noise ratio, attain three orders of magnitude in the MWC 17 spectrum! Weak emissions, which are hardly distinguishable from noise, make it difficult to generate the continuum. Absorptions, by contrast, (except for depressions in the emission lines) are presented by the interstellar Na I(1) lines, strongest DIBs, and, possibly, by the $H\delta$ photospheric wings. With regard to these circumstances, we detected only small variations of the intensities of the lines and profile shapes and positions with time. The strongest emissions were on September 2, 2006; the residual intensities of the emission peaks in this spectrum are on the average 20% higher than in January and 30% higher than in March of the same year.

Heliocentric radial velocities, V_r , were found for the profiles on the whole or for separate details by combination of their direct and mirror images. When comparing V_r for the same lines in the spectra obtained on different dates, it should be taken into account that apart from random errors, systematic errors of the order of 1 km s^{-1} are also possible. Table 2 shows the examples of the comparison of our data with each other and with the data from [8]. The profile shape which is complex and changing from line to line does not allow us to confine ourselves to intensity and a single value of radial velocity only. These and additional profile parameters are collected in Tables 2, 3, 4, and 5. In these tables, r is the residual intensity of an emission peak or an absorption core, V/R is the ratio of residual intensities of the blue and red components for double-peaked emissions. The velocities are rounded to whole km s^{-1} , they correspond to:

¹<http://simbad.u-strasbg.fr/simbad/>

Table 2. Profile parameters (see in the text) for some lines and dates according to our measurements and Zickgraf's data [8] (in italics). Heliocentric velocities V_r are in km s^{-1} . Uncertain measurements are marked with a colon

Date	r	V/R	V_r	V_{em}	V_{abs}	$V(r/2)$	$V(r \approx 1)$			
[O I] 6300										
Nov 15, 2005	33	0.94	-48	-59	-38	-51	-74	-23	-92	0
Sep 02, 2006	33	0.97	-48	-57	-40	-49	-75	-24	-95	-5
	<i>25</i>	<i>0.91</i>	<i>-47:</i>	<i>-59</i>	<i>-39</i>	<i>-51</i>	<i>-72:</i>	<i>-21:</i>	<i>-92:</i>	<i>-2:</i>
[Fe II] 5334										
Nov 15, 2005	3.7		-48				-72	-26	-95:	3:
Jan 15, 2006	3.7		-46				-71	-24	-94:	-1:
Jan 16, 2006	4.2		-47				-72	-23:	-95:	0:
Mar 14, 2006	3.7		-46				-72	-26:	-93:	-5:
Sep 02, 2006	4.9		-47				-72	-28	-94:	-5:
[N II] 5755										
Nov 15, 2005	16	0.84	-47	-65	-32	-52	-85:	-16	-125:	5
Jan 15, 2006	14	0.82	-47	-64	-31	-53	-86:	-15	-125:	6
Jan 16, 2006	15	0.80	-47	-64	-32	-55	-85:	-15:	-124:	10:
Sep 02, 2006	21	0.80	-48	-64:	-32	-52	-83:	-17	-120:	7:
Fe II 5169										
Jan 15, 2006	5.7	0.74	-42	-55:	-36	-50:	-69:	-16	-98:	2:
Jan 16, 2006	6.7	0.72	-41	-55:	-37	-51:	-71:	-18	-102:	0:
Mar 14, 2006	4.6	0.78	-43	-57:	-35	-51:	-71:	-19:	-97:	5:
Fe II 5316										
Nov 15, 2005	13	1.00	-51	-69	-35	-50	-88	-13	-112	11
Jan 15, 2006	11	0.95	-51	-68	-37	-51	-88	-14	-115:	12:
Jan 16, 2006	12	0.94	-51	-69	-36	-52	-88	-14:	-111:	14:
Mar 14, 2006	10	1.07	-52	-70	-33	-52:	-90:	-13:	-115:	14:
Sep 02, 2006	15	1.12	-54	-70	-34	-49	-90	-15	-108:	11
Fe II 6318										
Nov 15, 2005	8.5	0.94	-50		-34	-50	-86	-13	-105:	8:
Sep 02, 2006	9.1		-53		-39		-89	-15	-105:	8:
[S III] 6312										
Nov 15, 2005	4.0	0.73	-47:		-25		-81:	-12	-118:	10:
Sep 02, 2006	5.3	0.68	-46:	-66:	-28	-50	-80:	-14	-122:	6:
	<i>3.1</i>	<i>0.76</i>	<i>-50:</i>	<i>-70</i>	<i>-25</i>	<i>-44</i>	<i>-88:</i>	<i>-12:</i>	<i>-123:</i>	<i>4:</i>

Table 2. (Contd.)

Date	r	V/R	V_r	V_{em}	V_{abs}	$V(r/2)$	$V(r \approx 1)$			
He I 5876										
Nov 15, 2005	7	0.82	-54	-78:	-28	-52:	-108	-6	-145:	25
Jan 15, 2006	6	0.76	-50	-70:	-27	-57:	-110	-3	-142:	33:
Jan 16, 2006	6	0.75	-48:		-26		-106:	-3:	-150:	33
Sep 02, 2006	9	0.75	-56	-80:	-33		-110	-11	-140:	20:
	6	0.68	-50:	-78	-24	-57	-105:	0:	-135:	30:
He I 6678										
Nov 15, 2005	2.3	0.84	-51	-72	-23	-60:	-106:	-1:	-138:	20:
Sep 02, 2006	2.7	0.78	-54:		-28:		-105:	-2:	-135:	22:
				-67	-20	-53				
H α										
Nov 15, 2005				-105:	-10	-54				
Sep 02, 2006				-100:	-13	-55				
				-101	-11	-59				

- V_r —the upper part of the whole profile for the emission or the lower part of the absorption component;
- V_{em} —the emission peaks of a double-peaked profile;
- V_{abs} —the depression in the upper part of the emission line profile;
- $V(r/2)$ —the shortwave and longwave (hereinafter “blue” and “red”) slopes of the emission line profile at the half maximum intensity;
- $V(r \approx 1)$ —the blue and red boundaries of the emission at the bottom of the profile.

The results from [8] are given in italics. Table 3 gives the velocities measured from the Na I(1) absorption components.

As follows from Table 2, the variations of radial velocities for strong emissions [O I] with distinct profiles in our two spectra, and the discrepancy with the data from [8] do not go beyond the measurement error. The same can be said about the weaker [N II] and [Fe II] emissions. Velocity variations from spectrum to spectrum for other lines are notable. They are mainly due to the variations in the red regions of the profiles (the shifts of their red slopes and peaks). The shifts for the [S III] and Fe II emissions are about 2–3 km s⁻¹, for He I 5876 Å they attain 5 km s⁻¹.

Red regions are also most variable in the complex absorption/emission profiles of the Na I doublet. Figure 1 shows the result of averaging the profiles of the Na I 5896 Å line using several our spectra. The emission component is presented in this figure only by its blue region (V_r of -60 km s⁻¹), its red region is overlapped by interstellar extinction. Table 3 shows

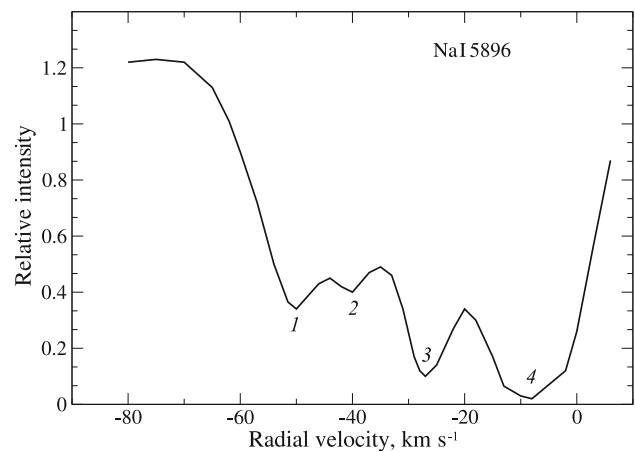


Fig. 1. Profile of the Na I 5896 Å line in the spectrum of MWC 17 averaged over all available spectra. Numbers 1–4 denote the positions of four profile components from Table 3.

Table 3. Radial velocities V_r measured for the components of the Na I doublet D-lines for certain dates. Zickgraf’s measurements are given in italics [8]

Date	V_r , km s ⁻¹			
	1	2	3	4
Na I 5890				
Nov 15, 2005	-52	-40	-25	-14
Jan 15, 2006	-50	-38	-27	-8
Jan 16, 2006	-50	-38	-27	-9
Sep 02, 2006	-50	-38	-28	-9
	<i>-52</i>	<i>-41</i>	<i>-25</i>	<i>-13</i>
Na I 5896				
Nov 15, 2005	-50	-40	-25	-12
Jan 15, 2006	-50	-40	-27	-9
Jan 16, 2006	-50	-41	-27	-8
Sep 02, 2006	-53	-42	-26	-9
	<i>-49</i>	<i>-42</i>	<i>-25</i>	<i>-11</i>

that three blue components of the Na I 5896 Å line keep their positions while the red component is shifted on November 15, 2005 by $-(5-6)$ km s⁻¹ relative to its position in 2006.

The double-peaked H α emission profile is of type III according to the Beals classification [14]. The position of emission peaks $V_r \approx -100$ and -12 km s⁻¹ as well as the position of the absorption $V_r \approx -55$ km s⁻¹ are almost constant both in our two spectra of 2005, 2006 and in the earlier spectrum by Zickgraf [8]. One can see the change in the strongest emission intensities as compared with the data from [8] (see Table A1 in that paper). Both the [O I] 6300 Å and [S III] 6312 Å lines with an excitation potential of 3.3 eV are 30% stronger in our spectrum than those in [8]. The He I 5876 Å line has scarcely varied as compared with the measurements by Zickgraf [8].

Table 4 and Fig. 2 illustrate the hierarchy of emission profiles by width and degree of asymmetry: both increase from top lines of the table to the bottom. The velocities in this table are averaged for the groups of lines with a similar profile shape. They can be useful not only in estimating the structure and kinematics of the MWC 17 envelope but also in controlling the line identification accuracy. As mentioned in previous studies of MWC 17 (and which is commonly characteristic of B[e] stars), the narrowest lines in the optical

spectrum are the forbidden emissions [Fe II] and [O I]. Both are almost symmetrical. The former ones have sharper peaks (bifurcation is notable only in some lines and in some our spectra), the latter ones have more distinctly forked peaks. The red peak of the [O I] profile is stronger than the blue one.

In accordance with the results from [8], such a ratio of peak intensities is amplified for the H, He I, and [S III] lines. According to our data, it is also typical of [N II], [O III], [Fe III] and generally of most emissions. An exception is provided by the Fe II lines of low excitation (e.g., Fe II (49,48) 5316 Å, see Table 2), the blue component of which can be stronger than the red one.

The permitted Fe II emissions are notably broader than the forbidden ones, and they are slightly asymmetric: the blue slope is steeper than the red one. The low and high-excitation Fe II lines (about 3 and 10 eV respectively) noticeably differ by the shape of the profile upper part: it is close to rectangular for the latter ones (e.g., the Fe II 6318 Å line profiles in Table 2), the central depression is not distinct. Difference in widths of the permitted and forbidden emissions indicate that these groups of lines form in different physical conditions.

The members of the 42nd Fe II multiplet, which is the strongest in the visible spectrum, stand out for their profile shape. They are as broad as the other Fe II emissions but abruptly get narrow toward the tops due to intensity decrease in the blue half of the line. As can be seen from Table 4 and Fig. 2, the positions of the red emission peak and the whole red slope of the profile are almost the same as in other Fe II lines; the blue peak is weak and shifted toward the red region, it is faintly visible on the blue slope which is much smoother than the red one. Such asymmetry (the blue peak is not distinct and is weaker than the red one, the blue slope is smoother than the red one) is as well characteristic of emissions of forbidden ions [N II], [S III], and [Fe III] which are broader at the bottom. It also remains in the broadest (exclusive of those of hydrogen) He I and [O III] lines. Among the model profiles [8], those are the most similar to the observed spectrum of MWC 17 which are computed for a tilted disk ($i \approx 45^\circ$). Zickgraf [8] considers that $i \approx 80^\circ$ for MWC 17.

Table 5 shows part of the identified lines and their parameters.² As the discrepancies in the parameters from spectrum to spectrum for most lines are small, each line is presented by a single set of the parameters. In the wavelength interval 4050–4570 Å, the parameters were obtained from the spectrum of

²The complete list is available in the e-preprint <http://www.arxiv.org/abs/1511.07700>.

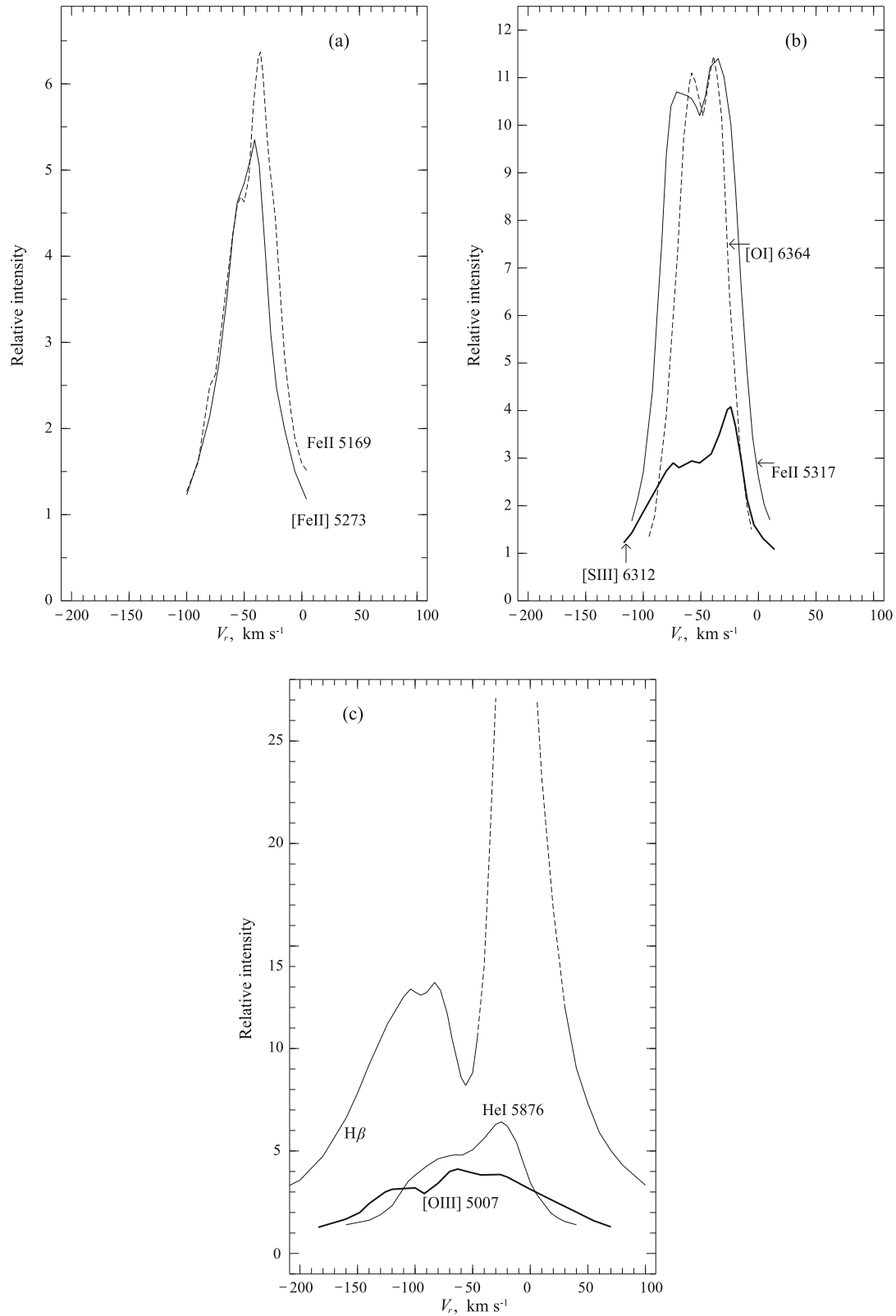


Fig. 2. Profiles of the representative lines in the MWC 17 spectrum: (a) Fe II 5169 Å (dashed line) and [Fe II] 5273 Å (solid); (b) Fe II 5317 Å (thin solid line), [S III] 6312 Å (thick solid), and [O I] 6364 Å (dashed); (c) [O III] 5007 Å (thick solid line), He I 5876 Å (thin solid), and H β (thin solid, prolonged with the dashed line at high intensities).

Table 4. Mean heliocentric radial velocities for emission groups in the MWC 17 spectrum with a similar profile shape. Designations are the same as for Table 2. Uncertain measurements are marked with a colon

Line type	V_r	V_{em}		V_{abs}	$V(r/2)$		$V(r \approx 1)$	
[Fe II]	-47	-53:	-42:	-50	-72	-26	-95	-5:
[O I], [S II]	-48	-58	-39	-50	-74	-24	-93	-4
Fe II low exc.	-51	-71	-34	-49	-89	-11	-105:	9
Fe II high exc.	-51	-63:	-36:	-49:	-87	-14	-105:	9:
Fe II(42)	-42	-55:	-36	-50:	-70	-18	-103:	5:
[N II], [S III]	-47	-64	-30	-52	-83	-15	-120:	8:
He I	-53:	-76:	-28:	-55:	-108:	-6:	-142:	25:
[O III]	-55:	-100:	-50:	-78:	-130:	20:	-180:	90:
H α , H β	-52:	-95:	-12	-55				

March 14, 2006; in longer wavelength intervals, they were found by averaging two or more spectra. As follows from Table 5, we have not detected any absorptions in the MWC 17 spectrum with all the high-quality material in the broad wavelength interval. Using spectra with a resolution limit of 1.3 Å, Jaschek and Andriolat [15] found several absorptions forming in the stellar atmosphere: Al II 6066, S II 6102, N II 6632, and C II 6800 Å. We have not detected the first three absorptions, which could occur in our spectral interval.

4. LOCATION OF MWC 17 IN THE GALAXY

If not particularly the radial velocity of the star itself (it may be peculiar), then at least the presence of the blue-shifted components in the interstellar Na I(1) lines with velocities of up to -50 km s^{-1} (there is even a weak component with a velocity of about -60 km s^{-1}) says that MWC 17 is located in the Perseus Arm or behind it. The distance to MWC 17 can be estimated by different methods, but the peculiarity of the object make all them unreliable.

- Spectrophotometric parallax. The absence of photospheric absorptions in the star's spectrum makes the accepted $(B - V)_0$ color index uncertain. Martel and Gravina [16] give the following for MWC 17: $V = 11^m 66$, $(B - V) = 0^m 42$; along with this, for early subtype B we obtain the color excess $E(B - V) \approx 0^m 65$ and visual brightness extinction $A_V \approx 2^m 5$. Let us notice that we obtain a smaller excess $E(B - V) \approx 0^m 4$ using the measured equivalent width of the interstellar band $W(5780) \approx 0.2 \text{ \AA}$ and correlation

$W(5780) - E(B - V)$ from [17]. Even with $M_V \approx -4^m$ (such a luminosity would rather correspond to a star from the upper part of the main sequence than to a supergiant), $d \approx 4 \text{ kpc}$. It is the lower limit of the MWC 17 distance. However, the estimates of both the star's color and its spectral type are unreliable until the distorting influence of emissions is taken into account and photospheric lines are detected. However, if we bear in mind that according to Miroshnichenko [18], the visual magnitude of the star $V \approx 13^m$, then the distance to it will be considerably greater.

- According to [19], the interstellar extinction toward MWC 17 reaches $2^m 5$ at a distance of 1 kpc and remains almost the same up to 3–4 kpc. If we assume the above estimated $A_V \approx 2^m 5$ for MWC 17, we will obtain only a limitation on the object's distance, $d > 1 \text{ kpc}$.
- Among the velocities given in Table 4, the closest to V_{sys} can be the velocities of the forbidden emissions: -47 km s^{-1} ($V_{Isr} = -42 \text{ km s}^{-1}$). By Brand and Blitz [20], a distance $d \geq 2 \text{ kpc}$ corresponds to this value.

There is an important additional point: in the sky, MWC 17 is located at the southern boundary of the compact association Cas OB8 ($d \approx 2.9 \text{ kpc}$ from [21]). For the member of this association HD 9311, $V_r = -42 \text{ km s}^{-1}$; the structure of the interstellar Na I lines in its spectrum is similar to that in the MWC 17 spectrum ($V_r \approx -(65-50)$, -14 km s^{-1} [22]). Obviously, the question on possible membership of MWC 17 in Cas OB8 is a key one for determination of the distance and origin of the object.

Table 5. Central residual intensities and heliocentric radial velocities for the lines in the MWC 17 spectrum. Designations are the same as in Table 2. Uncertain measurements are marked with a colon. The complete table is available in the e-preprint <http://www.arxiv.org/abs/1511.07700>

Ident.	λ , Å	r	V_r	V_{em}		V_{abs}	$V(r/2)$		$V(r \approx 1)$	
[S II] 1F	4068.60	4.6	-48:				-77:	-22:	-98:	-5:
[S II] 1F	4076.35	2.7:	-47:							
H δ	4101.74	5.9			-23	-61:				
Fe II(28)	4178.85	2.7	-48	-67:	-24:	-46	-90:	-7:	-100:	7:
Fe II(27)	4233.17	4.8	-50	-68:	-35	-49	-84:	-21:	-105:	10
[Fe II] 21F	4243.98	2.6:	-47:							
[Fe II] 21F	4276.83	3.1:	-50							
[Fe II] 7F	4287.39	7.1	-48	-57	-42	-52	-72:	-26:	-95:	5:
[Fe II] 21F	4319.62	2.1	-48:							
H γ	4340.47	14.0			-21:	-58				
[Fe II] 7F	4359.33	5.6	-46					-25:		0:
Fe II(32)	4413.59									
[Fe II] 7F	4413.78	4.6	-50				-74:	-27:	-111:	-3:
[Fe II] 6F	4416.27	4.3								
[Fe II] 7F	4452.10	3.4	-48	-57:	-40	-50:	-74:	-26:	-98:	-4:
[Fe II] 6F	4457.94	2.6	-47	-60:	-40:	-52:	-74:	-28:	-102:	-7:
He I(14)	4471.52	2.3	-48:	-82:	-29:	-59:	-105:		-142:	
[Fe II] 7F	4474.90	2.4	-49:				-80:	-22:	-108:	-3:
Fe II(37)	4491.40	2.0:	-53:	-73:	-31:	-52:	-92:		-105:	
Fe II(38)	4508.28	2.0	-50	-72:	-37	-51:			-92:	8:
Fe II(37)	4515.33	3.4	-51	-67	-28:	-49:	-87:	-18:		
Fe II(37)	4520.22	3.4	-50	-69:	-27:	-45:	-89:	-8:	-106:	
Fe II(38)	4522.63	3.4	-51	-65	-33:	-49:	-81:	-19:	-102:	7
Fe II(38)	4549.47	3.1	-51	-70:	-32:	-50:	-87:	-15:	-107:	0:
Ti II(82)	4549.63									
Fe II(37)	4555.89	3.6	-50	-72:	-30	-45	-89:	-13:	-107:	2:
Fe II(38)	4576.33	2.1	-50:							
Fe II(38)	4583.83	6.5	-49	-70	-35	-51:	-87	-10		13:
Fe II(37)	4629.33	6.0	-50	-71	-35:	-51:	-88	-10:	-109:	12:
[Fe II] 4F	4639.67	2.5	-49:		-47:		-75:	-28:	-90:	-10:
[Fe III] 3F	4658.1	7.0	-46	-67:	-21	-49:	-91:	-7:	-122:	16
Fe II(37)	4666.75	2.0	-49:	-68:	-22:				-123:	3:
[Fe III] 3F	4701.5	2.6:	-46:	-68:	-17:	-45:	-92:	-4:	-108:	14:

Table 5. (Contd.)

Ident.	$\lambda, \text{\AA}$	r	V_r	V_{em}		V_{abs}	$V(r/2)$		$V(r \approx 1)$	
He I(12)	4713.18	1.5:	-49:	-88 :	-20:	-52:				
[Fe II]4F	4728.07	4.0:	-46	-53 :	-42:	-48:	-69:	-26:	-94:	0:
Fe II(43)	4731.47	1.7:	-51:						-95:	-4:
[Fe III]3F	4733.9	1.8:	-48:	-60 :	-24:	-42:				
[Fe III]3F	4754.7	2.0	-48:	-75 :	-23:	-55:			-112:	20:
[Fe III]3F	4769.4	1.7:	-43:	-63 :	-18:	-44:			-95:	10:
[Fe II]20F	4774.72	2.2	-48				-69:	-25:	-94:	-8:
[Fe III]3F	4777.7	1.3:	-51:	-65 :	-23:	-42:			-114:	23:
[Fe II]20F	4814.53	4.8:	-46	-56 :	-42:	-52:	-75:	-24:	-102:	5:
Cr II(30)	4824.14	1.3:	-46:	-69 :	-23:	-50:			-104:	9:
H β	4861.33	12.0:				-96:				
					-15	-56				
[Fe II]20F	4874.48	2.1	-47				-74:	-24:	-90:	0:
[Fe II]4F	4889.62	4.8	-47	-54:	-42:	-50:	-70:	-26:	-98:	-1:
[Fe II]	4898.61	2.2	-48						-90:	-16:
[Fe II]20F	4905.34	3.0	-47	-53:	-41:	-49:	-73:	-23:	-98:	0:
He I(48)	4921.93	2.1:	-51:	-101:	-25:				-115:	
Fe II(42)	4923.92	6.0	-43:	-55	-36	-50	-75	-17	-103:	8:
[Fe III]1F	4930.5	1.7	-42:	-69:	-18:	-55:	-83:	5:	-106	25:
[Fe II]20F	4947.37	1.8	-45:						-80:	
[Fe II]20F	4950.74	1.9	-45				-64:	-27	-83:	-8:
[O III]1F	4958.92	2.0	-48:				-127:	21:	-170:	90:
[Fe II]20F	4973.39	2.1	-48	-58:	-40:	-47:	-70:	-26	-90:	-8:
[O III]1F	5006.84	4.0	-56:	-100:	-50:	-78:	-130:	19:	-183:	95:
[Fe III]1F	5011.3	2.5	-46	-60:	-22	-48:	-92:	-9:	-119:	20:
He I(4)	5015.68	3.6	-47:	-73:	-23	-46:		-2:	-120:	20:
Fe II(42)	5018.44	6.5	-43	-55	-37	-51:	-72:	-20	-108:	6:
[Fe II]20F	5020.23	2.0:	-45:		-40:	-46:				
Fe II	5030.64	1.8:	-45:	-62:	-37	-53:	-70:	-22:	-93:	-5:
Si II(5)	5041.03	2.1	-46				-78:	-18:	-110:	2:
[Fe II]20F	5043.52	1.6	-46						-85:	-11:
He I(47)	5047.74									
[Ti II]19F	5047.91	2.0	-45:							

Meanwhile, we have to assume that the distance to MWC 17 can be of the order of both 4–5 kpc and 2–3 kpc—in the case there is some additional (possibly circumstellar) extinction.

The profile of the Na I D lines in the MWC 17 spectrum is close to that observed in the spectrum of the hot B-type star—the optical component of the IR source IRAS 00470+6429, which is located near the galactic plane and has the coordinates $\alpha(2000) = 00^{\text{h}}50^{\text{m}}06^{\text{s}}.0$, $\delta(2000) = +64^{\circ}45'35''$, $l = 122^{\circ}.8$, and $b = 1^{\circ}.9$. In the optical spectrum of its central star, there are two interstellar components of the Na I D lines [7]. Heliocentric radial velocities in the IRAS 00470+6429 spectrum (about -62 and -13 km s^{-1}) coincide with those in the MWC 17 spectrum. In the spectra of both objects, the positions of diffuse interstellar bands are also similar: $V_r(\text{DIB}) \approx -14 \text{ km s}^{-1}$.

5. CONCLUSIONS

High quality of the spectral material which we used allowed us to identify spectral features in detail. The thorough search has not led to detection of any absorptions in the MWC 17 spectrum which emerge in the stellar atmosphere. Out of absorption details, only interstellar components of the Na I D lines and DIBs were identified. The DIBs are weak, their equivalent widths are $W(5780) \approx 0.2 \text{ \AA}$ and $W(5797) \approx 0.15 \text{ \AA}$.

As a systemic velocity, V_{sys} , the velocity for forbidden emissions can be accepted: -47 km s^{-1} (relative to the local standard $V_{\text{lsr}} = -42 \text{ km s}^{-1}$).

Comparison between our results and the measurements of Zickgraf [8] allows us to draw an inference on the absence of significant variability of spectral details.

We noticed variations of radial velocities from spectrum to spectrum which are small and can hardly give sure evidence on spectroscopic binarity of MWC 17. In order to solve this problem, observations of this star with high positional accuracy should be continued. Taking into account high intensity of the emission details in the spectrum of this faint star, such observations can be also made on telescopes of a moderate diameter.

ACKNOWLEDGMENTS

The authors are grateful to V. E. Panchuk and M. V. Yushkin for considerable assistance with the observations on the BTA. The study was performed with the support of the Russian Foundation for Basic

Research (project 14-02-00291 a). The observations on the 6-m telescope of the Special Astrophysical Observatory are conducted with the support of the Ministry of Education and Science of the Russian Federation (agreement № 14.619.21.0004, project ID RFMEFI61914X0004). The astronomical databases SIMBAD and ADS were used in the study.

REFERENCES

1. D. A. Allen and J. P. Swings, *Astron. and Astrophys.* **47**, 293 (1976).
2. P. S. Th e, D. de Winter, and M. R. P erez, *Astron. and Astrophys. Suppl.* **104**, 315 (1994).
3. H. J. G. L. M. Lamers, F. J. Zickgraf, D. de Winter, et al., *Astron. and Astrophys.* **340**, 117 (1998).
4. A. S. Miroshnichenko, *Astrophys. J.* **667**, 497 (2007).
5. M. Kraus, M. Borges Fernandes, and O. Chesneau, *ASP Conf. Ser.* **435**, 395 (2010).
6. D. M. Kelly and B. J. Hrivnak, *Astrophys. J.* **269**, 1040 (2005).
7. A. S. Miroshnichenko, E. L. Chentsov, V. G. Klochkova, et al., *Astrophys. J.* **700**, 209 (2009).
8. F.-J. Zickgraf, *Astron. and Astrophys.* **408**, 257 (2003).
9. V. Panchuk, V. Klochkova, M. Yushkin, and I. Najdenov, *J. Optical Technology* **76**, 87 (2009).
10. V. E. Panchuk, M. V. Yushkin, and I. D. Najdenov, Preprint No. 179 (Special Astrophysical Observatory, Nizhny Arkhyz, 2003).
11. M. V. Yushkin and V. G. Klochkova, Preprint No. 206 (Special Astrophysical Observatory, Nizhny Arkhyz, 2005).
12. V. G. Klochkova, V. E. Panchuk, M. V. Yushkin, and D. S. Nasonov, *Astrophysical Bulletin* **63**, 386 (2008).
13. P. W. Merrill and C. G. Burwell, *Astrophys. J.* **78**, 87 (1933).
14. C. S. Beals, *Publ. Dominion Astrophys. Obs.* **9**, 1 (1953).
15. C. Jaschek and Y. Andri at, *Astron. and Astrophys. Suppl.* **136**, 53, (1999).
16. M. T. Martel and R. Gravina, *IBVS*, No. 2750 (1985).
17. S. D. Friedman, D. G. York, B. J. McCall, et al., *Astrophys. J.* **727**, 33 (2011).
18. A. S. Miroshnichenko, private communication.
19. Th. Neckel, G. Klare, and M. Sarcander, *Astron. and Astrophys. Suppl.* **42**, 251 (1980).
20. J. Brand and L. Blitz, *Astron. and Astrophys.* **275**, 67 (1993).
21. R. M. Humphreys, *Astrophys. J. Suppl.* **38**, 309 (1978).
22. G. M unch, *Astrophys. J.* **125**, 42 (1957).

Translated by N. Oborina